VIP Superparamagnetism Very Important Paper

Deutsche Ausgabe: DOI: 10.1002/ange.201603406
Internationale Ausgabe: DOI: 10.1002/anie.201603406

Hydrogen Treatment for Superparamagnetic VO_2 Nanowires with Large Room-Temperature Magnetoresistance

Zejun Li[+], Yuqiao Guo[+], Zhenpeng Hu, Jihu Su, Jiyin Zhao, Junchi Wu, Jiajing Wu, Yingcheng Zhao, Changzheng Wu, and Yi Xie*

Abstract: *One-dimensional (1D) transition metal oxide (TMO) nanostructures are actively pursued in spintronic devices owing to their nontrivial d electron magnetism and confined electron transport pathways. However, for TMOs, the realization of 1D structures with long-range magnetic order to achieve a sensitive magnetoelectric response near room temperature has been a longstanding challenge. Herein, we exploit a chemical hydric effect to regulate the spin structure of 1D V–V atomic chains in monoclinic VO_2 nanowires. Hydrogen treatment introduced V^{3+} ($3d^2$) ions into the 1D zigzag V–V chains, triggering the formation of ferromagnetically coupled V^{3+}–V^{4+} dimers to produce 1D superparamagnetic chains and achieve large room-temperature negative magnetoresistance (−23.9 %, 300 K, 0.5 T). This approach offers new opportunities to regulate the spin structure of 1D nanostructures to control the intrinsic magnetoelectric properties of spintronic materials.*

One-dimensional (1D) nanomaterials, which benefit from strong charge and spin coupling and facile chemical modification, are promising materials for next-generation spintronic devices owing to their sensitive magnetoelectric response.[1] In fact, large magnetoresistance (MR), which is at the heart of spintronic devices, has been realized in 1D confined materials. For example, 1D organic molecular wires embedded within zeolites show exceptionally large MR at room temperature and low fields, where the very high MR value is a result of the confinement of the current path along the 1D chain.[2] 1D graphene nanoribbons also exhibit very large MR in low magnetic fields because of the formation of cyclotron orbits and delocalization effects in the presence of an external magnetic field.[3] Compared with the previously reported sp electron systems of 1D molecular wires and graphene nanoribbons, 3d transition-metal oxides (TMOs) typically exhibit strong interactions between electron carriers and magnetism to enable effective spin transport.[4] However, the lack of 1D chains with intrinsic magnetic order in TMOs greatly hampers the development of new 1D systems that exhibit rich magnetoelectronic properties and large MR effects.

Single-domain VO_2 nanowires as a prototype of strongly correlated TMOs comprising infinite 1D V–V atomic chains provide a promising long-range-order 1D chain for regulating the spin configuration. VO_2 undergoes a well-known metal–insulator transition (MIT) near room temperature ($T_{MIT} \approx 340$ K) with an accompanying structural transition of the V–V atomic chains.[5] Across the MIT, the 1D linear vanadium chains are transformed into zigzag chains, as illustrated in the Supporting Information, Figure S1. As a typical correlated material, there are various types of competing states in VO_2 nanowires, and their delicate balance renders the 1D V–V atomic chains sensitive to external perturbations, such as strain and electric, thermal, and optical fields.[6] However, the magnetoelectronic response of the 1D V–V atomic chains in VO_2 has thus far represented an enormous challenge, perhaps as a consequence of the practical difficulty of spin-arrangement tuning in the nonmagnetic singlet spin configuration of monoclinic zigzag V atom chains[7] (see Figure 3 a). Therefore, actively controlling and manipulating the spin configuration along 1D V–V atomic chains is a promising approach for achieving unique spin-related magnetoelectronic properties and even large MR in 1D TMO systems.

Herein, we exploit a hydric effect to regulate the spin structure of 1D V–V atomic chains in VO_2 nanowires, as a new 1D superparamagnetic structure, resulting in an extraordinarily large negative MR for the monoclinic VO_2 (M_1) nanowires at room temperature. Hydrogen treatment of VO_2 (M_1) nanowires successfully introduces oxygen vacancies and V^{3+} ($3d^2$) ions into the 1D zigzag V–V chains, triggering the formation of ferromagnetically coupled V^{3+}–V^{4+} dimers and the transition from nonmagnetic to superparamagnetic chains (see Figure 1 a), which results in a large intrinsic negative MR (−23.9 %, 0.5 T, 300 K) owing to spin-polarized electron hopping. The large MR effect in our hydrogen-treated VO_2 nanowires was rationalized based on a novel magnetotransport model with strong coupling between structure, spin, and charge for 1D electron transport.

The 1D spin structure of the VO_2 nanowires was chemically modified by controlled annealing in hydrogen gas (see the Supporting Information, Section S2). These hydrogen-treated VO_2 nanowires were different from those described in previous work,[8] and subjected to systemic characterization, which confirmed the introduction of oxygen vacancies and V^{3+} ions during the hydrogen gas treatment (Section S3 and

[*] Z. J. Li,[+] Y. Q. Guo,[+] J. H. Su, J. Y. Zhao, J. C. Wu, J. J. Wu, Y. C. Zhao, Prof. C. Z. Wu, Prof. Y. Xie
Hefei National Laboratory for Physical Sciences at the Microscale
CAS Center for Excellence in Nanoscience, and CAS Key Laboratory of Mechanical Behavior and Design of Materials
University of Science & Technology of China
Hefei 230026 (P.R. China)
E-mail: czwu@ustc.edu.cn
Prof. Z. P. Hu
School of Physics, Nankai University
Tianjin 300071 (P.R. China)

[+] These authors contributed equally to this work.

Supporting information for this article can be found under: http://dx.doi.org/10.1002/anie.201603406.

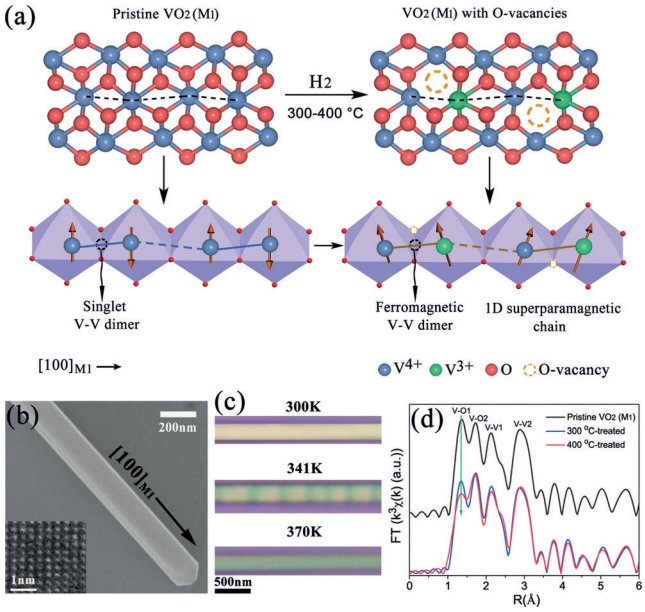

Figure 1. a) The 1D superparamagnetic chains in VO_2 (M_1) nanowires formed upon hydrogen treatment. b) SEM image of a hydrogen-treated VO_2 nanowire. Inset: HRTEM image of a hydrogen-treated VO_2 nanowire. c) Optical images of the domain evolution of a hydrogen-treated VO_2 nanowire. d) Fourier transforms of the V K-edge EXAFS oscillations of pristine and hydrogen-treated VO_2.

Figure S3). Figure 1b shows field-emission scanning electron microscopy (FESEM) and high-resolution transmission electron microscopy (HRTEM) images of representative hydrogen-treated VO_2 nanowires, which demonstrate that the nanowires maintained a uniform surface as well as a high degree of crystallinity after annealing in hydrogen gas. The evolution of the domain structure with increasing temperature features the typical MIT transition of VO_2, as shown in Figure 1c, indicating that the VO_2 nanowires still undergo this process after hydrogen treatment.[9]

Synchrotron radiation X-ray absorption fine structure (XAFS) analysis was conducted to further characterize the hydrogen-treated VO_2 nanowires. As illustrated in Figure 1d, all Fourier transform (FT) curves of the V K-edge EXAFS of pristine VO_2 (M_1) and hydrogen-treated samples exhibit four obvious peaks: two peaks (labeled as V–O1 and V–O2) at about 1.2 and 1.6 Å, which correspond to the V–O chemical bonds, and two peaks at approximately 2.2 and 2.9 Å, which are associated with V–V bonds (V–V1 and V–V2),[10] suggesting that the VO_2 samples keep their monoclinic phase after the hydrogen treatment. It should be noted that the intensity of the V–O1 peak decreased with an increase in the temperature of the hydrogen treatment, which indicates that the nearest-neighbor oxygen atoms around a vanadium atom are reduced during the annealing process. The results of the XAFS analysis clearly point towards the formation of oxygen vacancies in the hydrogen-treated VO_2 nanowires, which was further confirmed by XPS and ESR. The oxygen vacancies induced the formation of V^{3+} ions, resulting in the coexistence of V^{3+} ions and V^{4+} ions in hydrogen-treated VO_2 (Figure S4).

The spin configurations of pristine and hydrogen-treated VO_2 samples were determined by magnetometry to show how the magnetism is regulated in the hydrogen-treated VO_2 (M_1) nanowires, which revealed that room-temperature superparamagnetism was induced in our hydrogen-treated VO_2 (M_1). Pristine VO_2 (M_1) is known to be nonmagnetic; nevertheless, the field-dependent hysteresis loop (M–H) curve of pristine VO_2 (M_1) at 300 K demonstrated a weak paramagnetic-like behavior owing to Van Vleck paramagnetism[11] (Figure 2a). However, the S-shaped M–H curve for hydrogen-treated VO_2 demonstrates that this material is ferromagnetic at 300 K (Figure 2b). These different magnetic properties can be clearly seen in Figure 2c.

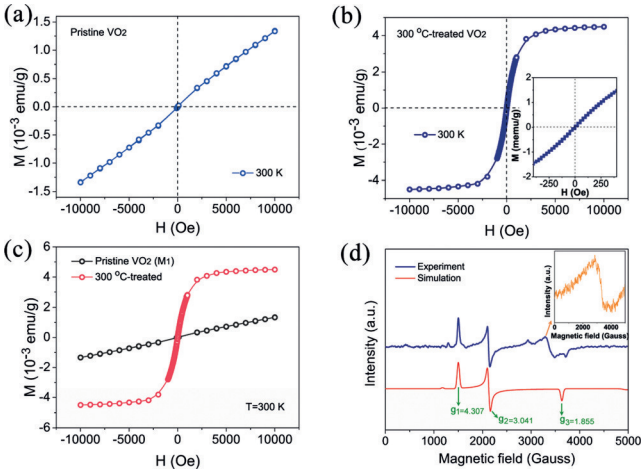

Figure 2. a, b) Field-dependent magnetization plots (M–H curves) for pristine and hydrogen-treated VO_2 nanowires at 300 K. c) Comparison of the M–H curves of pristine and hydrogen-treated VO_2 nanowires at 300 K. d) Experimental and simulated ESR spectra of hydrogen-treated VO_2 at 130 K.

The negligible remnant magnetization and coercivity in the hysteresis loops of treated VO_2 at 300 K (Figure 2b, inset) indicate superparamagnetic behavior similar to that usually observed in ferromagnetic nanoparticles, where the magnetization of a single nanoparticle can be regarded as one giant independent "spin".[12] As previously described, the V–V chain undergoes a transformation from rutile linear V–V atomic chains to monoclinic zigzag chain with V–V dimers, where the distance between neighboring dimers is relatively long. This configuration allows us to consider the total spin of a V–V dimer as a giant independent "spin". To further clarify the superparamagnetic-like behavior, the magnetic properties of our hydrogen-treated VO_2 sample at temperatures down to 4 K are illustrated in the Figure S6. ZFC measurements gave a weak peak at about 18 K as the blocking temperature (T_B), providing auxiliary evidence for the superparamagnetism. In this regard, we observed superparamagnetic behavior for our hydrogen-treated VO_2 (M_1), which therefore is a promising material for effective magnetoelectric modulation.

To probe the origin of the ferromagnetic exchange, further insight into the properties of hydrogen-treated VO_2 was

obtained by electron spin resonance (ESR) measurements. Figure 2d shows that no signal above the noise level was present for the parent control, and a new signal was observed for the hydrogen-treated samples. The orthorhombic principal g values were resolved as $g_1 = 4.307$, $g_2 = 3.041$, and $g_3 = 1.855$ and assigned to the higher spin state of $S_{total} = 3/2$, which originates from the ferromagnetic coupling pair between the V^{4+} ($3d^1$) and V^{3+} ($3d^2$) ions in hydrogen-treated VO_2 (M_1) (see Section S8 for details). These mixed-valence and exchange-coupled vanadium dimers (V^{3+}/V^{4+}) are consistent with the aforementioned magnetization measurements that suggested weak ferromagnetic behavior for hydrogen-treated VO_2 (M_1), which thus originates from the ferromagnetic coupling between the V^{4+} and V^{3+} ions, forming ferromagnetic V^{3+}–V^{4+} dimers with a giant "spin" of 3/2 (Figure 1a). However, the interactions between these giant "spins" are rather weak because of the long distances between neighboring ferromagnetic dimers, which results in negligible remnant magnetization and coercivity in the hysteresis loops. In this regard, the observed room-temperature ferromagnetism and increased susceptibility of hydrogen-treated VO_2 (M_1) could be ascribed to the ferromagnetic V^{3+}–V^{4+} dimers induced by hydrogen treatment (see Section S9 for details). Hence, these results reveal that V^{3+} ($3d^2$) ions are introduced into the VO_2 nanowires during the hydrogen reduction process, successfully inducing a superparamagnetic response at room temperature through the exchange interactions between V^{3+} ions and V^{4+} ions in the V–V dimers to form 1D spin-tunable V–V atomic chains.

The magnetotransport behavior of the VO_2 nanowires was investigated using four-terminal devices in a commercial physical property measurement system (Section S10). Figure 3a indicates that the pristine nonmagnetic VO_2 nanowires exhibited no appreciable MR effects. In contrast, the hydrogen-treated VO_2 (M_1) nanowires showed large negative MR at room temperature in low magnetic fields. Figure 3b shows the typical temperature-dependent resistivity of the hydrogen-treated VO_2 nanowires under different magnetic fields. Notably, the external magnetic field greatly suppresses the resistivity of the hydrogen-treated VO_2 (M_1) nanowires, resulting in a large negative MR effect. At 300 K, the negative MR values were as large as −13.8% at 0.05 T and −23.9% at 0.5 T. To further investigate the negative MR behavior, the field dependence of the MR for the hydrogen-treated VO_2 nanowires was determined. As shown in Figure 3c and Figure S8, the MR increases with the magnetic field, exhibiting obvious negative MR behavior. Furthermore, different MR behavior was observed in the high-temperature R-phase nanowire above T_{MIT}, where it displayed a positive MR effect (Figure S9). Figure 3d shows the temperature-dependent MR of the hydrogen-treated VO_2 nanowire; a positive–negative MR switch abruptly occurs at T_{MIT}, indicating the strong correlation of structure, spin, and charge in the 1D electron transport.

Density functional theory (DFT) calculations were also performed to understand how the room-temperature ferromagnetism of hydrogen-treated VO_2 (M_1) nanowires is induced by the incorporated V^{3+} ($3d^2$) ions. Figure 4a illustrates the spatial spin density distribution, where the red regions represent spin-up states and the blue regions represent spin-down states. This Figure clearly demonstrates that dimeric V ions exhibit the same spin state, indicating the intrinsic ferromagnetism in the reduced VO_2 (M_1) sample (for

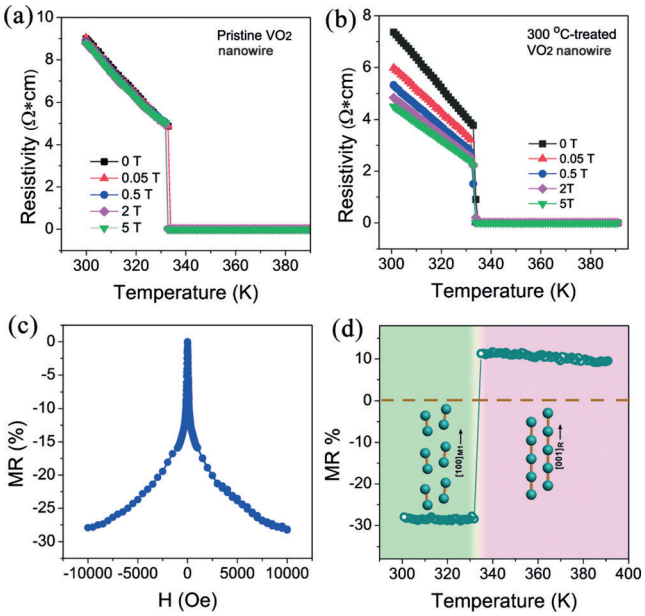

Figure 3. a, b) Temperature-dependent resistivity under various magnetic fields of pristine and hydrogen-treated VO_2 nanowires. c) Field-dependent MR of the hydrogen-treated VO_2 (M_1) nanowires at room temperature. d) Temperature-dependent MR of the hydrogen-treated VO_2 nanowires under a magnetic field of 0.5 T, clearly demonstrating the positive–negative MR transition at T_{MIT}. The MR value was calculated using MR [%] = $[R(H) - R(0)]/R(0)$.

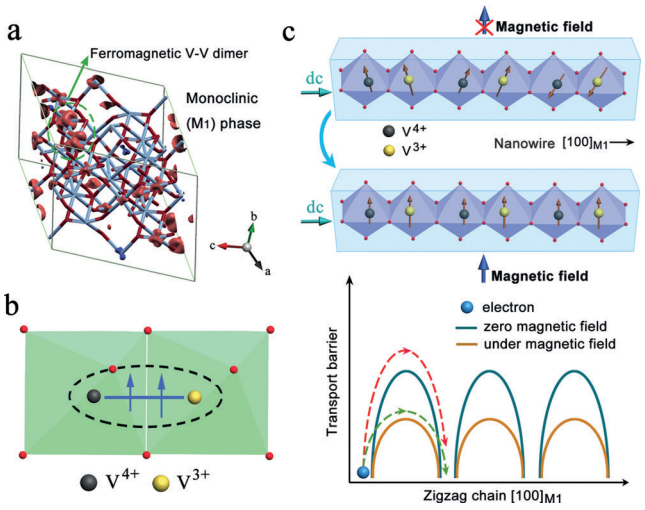

Figure 4. a) Calculated spatial spin density distribution; the red and blue regions represent spin-up and spin-down states, respectively. b) The ferromagnetic coupling between the V^{4+} ($3d^1$) and V^{3+} ($3d^2$) ions in the V–V dimer. c) Mechanism of the observed large negative MR effect in the hydrogen-treated VO_2 (M_1) nanowires.

details see Section S13), which is in good agreement with the results of the magnetic-property and ESR measurements.

Finally, the origin of the large negative MR in the hydrogen-treated VO_2 (M_1) nanowires at room temperature and in low magnetic fields was ascribed to spin-polarized electron hopping between ferromagnetic V^{3+}–V^{4+} dimers for 1D electron transport. Careful analysis of the field-dependent MR and magnetization at 300 K (Figure 3c, Figure 2b) helped us to understand the MR effect. The field-dependent MR curve exhibits two distinct regions, as shown in the Figure 3c: The MR rapidly increases in low magnetic fields of less than 0.25 T, whereas the MR changes slightly in higher fields of more than 0.25 T. Correspondingly, the field-dependent magnetization at 300 K (Figure 2b) also reaches saturation at approximately 0.25 T. The magnetization steeply increases in magnetic fields of less than 0.25 T, whereas the magnetization changes slowly in fields of >0.25 T. These results indicate that the MR and magnetization properties are closely related in both low and high fields (Figure S10); this striking feature revealed that the large negative MR is associated with the arrangement of the magnetic moments of the ferromagnetic V–V dimers in the presence of magnetic fields. In our case, as illustrated in Figure 4c, at zero field, the giant independent "spins" of the neighboring ferromagnetic dimers are distributed randomly. When a magnetic field is applied, the magnetic moments of the ferromagnetic dimers tend to rotate to align in parallel along the 1D V–V chain. As previously described, the conduction of monoclinic VO_2 is due to hopping transport.[13] The parallel alignment of the spins of the ferromagnetic dimers in a magnetic field reduced the barrier to electron hopping, resulting in decreased resistivity. Furthermore, the weak interactions of the ferromagnetic dimers allow the magnetic moments to rotate easily in low magnetic fields; thus the negative MR effect was pronounced in low magnetic fields, which is useful for practical applications.

In summary, the hydrogen treatment of 1D VO_2 (M_1) nanowires resulted in a system with large negative magnetoresistance. The introduction of V^{3+} ($3d^2$) ions into the VO_2 lattice framework induces the formation of ferromagnetic V^{3+}–V^{4+} dimers to produce 1D superparamagnetic chains, which resulted in an intrinsic large negative MR as high as $-23.9\,\%$ at 0.5 T and 300 K owing to spin-polarized electron hopping between these ferromagnetic dimers. Moreover, a novel magnetotransport phenomenon was observed in our hydrogen-treated VO_2 nanowires: A positive–negative MR transition occurred across the MIT, revealing the strong correlation of structure, spin, and charge for 1D electron transport. We anticipate that the chemical modification of 1D atomic chains will lead to new opportunities to trigger large MR effects and explore spin-related phenomena and functionalities in low-dimensional TMO systems.

Acknowledgements

We thank Dr. Lin-Jun Wang (USTC Center for Micro- and Nanoscale Research and Fabrication) for valuable discussions on the contact fabrication. We would like to thank beamline BL14W1 (Shanghai Synchrotron Radiation Facility) for providing the beam time. Some of this work was performed at the Steady High Magnetic Field Facilities, High Magnetic Field Laboratory, CAS. This work was financially supported by the National Basic Research Program of China (2015CB932302), the National Natural Science Foundation of China (21222101, 21501164, U1432133, 11321503, J1030412), the National Young Top-Notch Talent Support Program, the Chinese Academy of Sciences (XDB01020300), the Fok Ying-Tong Education Foundation, China (141042), the Fundamental Research Funds for the Central Universities (WK2060190027, WK2340000065, WK2310000055), and the Anhui Provincial Natural Science Foundation (1608085QA08).

Keywords: ferromagnetism · magnetoresistance · superparamagnetism · vanadium

How to cite: *Angew. Chem. Int. Ed.* **2016**, *55*, 8018–8022
Angew. Chem. **2016**, *128*, 8150–8154

[1] a) A. Fert, *Rev. Mod. Phys.* **2008**, *80*, 1517–1530; b) M. R. Li, M. Retuerto, Z. Deng, P. W. Stephens, M. Croft, Q. Huang, H. Wu, X. Deng, G. Kotliar, J. Sanchez-Benitez, J. Hadermann, D. Walker, M. Greenblatt, *Angew. Chem. Int. Ed.* **2015**, *54*, 12069–12073; *Angew. Chem.* **2015**, *127*, 12237–12241; c) J. Peng, Y. Guo, H. Lv, X. Dou, Q. Chen, J. Zhao, C. Wu, X. Zhu, Y. Lin, W. Lu, X. Wu, Y. Xie, *Angew. Chem. Int. Ed.* **2016**, *55*, 3176–3180; *Angew. Chem.* **2016**, *128*, 3228–3232.

[2] R. N. Mahato, H. Lülf, M. H. Siekman, S. P. Kersten, P. A. Bobbert, M. P. de Jong, L. De Cola, W. G. van der Wiel, *Science* **2013**, *341*, 257–260.

[3] J. Bai, R. Cheng, F. Xiu, L. Liao, M. Wang, A. Shailos, K. L. Wang, Y. Huang, X. Duan, *Nat. Nanotechnol.* **2010**, *5*, 655–659.

[4] a) L. Krusin-Elbaum, D. M. Newns, H. Zeng, V. Derycke, J. Z. Sun, R. Sandstrom, *Nature* **2004**, *431*, 672–676; b) Y. Tokura, N. Nagaosa, *Science* **2000**, *288*, 462–468.

[5] a) J. H. Park, J. M. Coy, T. S. Kasirga, C. Huang, Z. Fei, S. Hunter, D. H. Cobden, *Nature* **2013**, *500*, 431–434; b) N. B. Aetukuri, A. X. Gray, M. Drouard, M. Cossale, L. Gao, A. H. Reid, R. Kukreja, H. Ohldag, C. A. Jenkins, E. Arenholz, K. P. Roche, H. A. Durr, M. G. Samant, S. S. P. Parkin, *Nat. Phys.* **2013**, *9*, 661–666.

[6] a) B. Hu, Y. Ding, W. Chen, D. Kulkarni, Y. Shen, V. V. Tsukruk, Z. L. Wang, *Adv. Mater.* **2010**, *22*, 5134–5139; b) S.-H. Bae, S. Lee, H. Koo, L. Lin, B. H. Jo, C. Park, Z. L. Wang, *Adv. Mater.* **2013**, *25*, 5098–5103; c) K. Liu, C. Cheng, Z. Cheng, K. Wang, R. Ramesh, J. Wu, *Nano Lett.* **2012**, *12*, 6302–6308; d) T. S. Kasirga, D. Sun, J. H. Park, J. M. Coy, Z. Fei, X. Xu, D. H. Cobden, *Nat. Nanotechnol.* **2012**, *7*, 723–727.

[7] a) K. L. Holman, T. M. McQueen, A. J. Williams, T. Klimczuk, P. W. Stephens, H. W. Zandbergen, Q. Xu, F. Ronning, R. J. Cava, *Phys. Rev. B* **2009**, *79*, 245114; b) M. Nakano, K. Shibuya, D. Okuyama, T. Hatano, S. Ono, M. Kawasaki, Y. Iwasa, Y. Tokura, *Nature* **2012**, *487*, 459–462.

[8] J. Wei, H. Ji, W. Guo, A. H. Nevidomskyy, D. Natelson, *Nat. Nanotechnol.* **2012**, *7*, 357–362.

[9] J. Cao, E. Ertekin, V. Srinivasan, W. Fan, S. Huang, H. Zheng, J. W. L. Yim, D. R. Khanal, D. F. Ogletree, J. C. Grossman, J. Wu, *Nat. Nanotechnol.* **2009**, *4*, 732–737.

[10] a) T. Yao, X. Zhang, Z. Sun, S. Liu, Y. Huang, Y. Xie, C. Wu, X. Yuan, W. Zhang, Z. Wu, G. Pan, F. Hu, L. Wu, Q. Liu, S. Wei, *Phys. Rev. Lett.* **2010**, *105*, 226405; b) C. Wu, F. Feng, J. Feng, J.

Dai, L. Peng, J. Zhao, J. Yang, C. Si, Z. Wu, Y. Xie, *J. Am. Chem. Soc.* **2011**, *133*, 13798 – 13801.
[11] a) C. N. Berglund, H. J. Guggenheim, *Phys. Rev.* **1969**, *185*, 1022 – 1033; b) V. Eyert, *Ann. Phys.* **2002**, *11*, 650 – 704.
[12] a) C. Xiao, J. Zhang, J. Xu, W. Tong, B. Cao, K. Li, B. Pan, H. Su, Y. Xie, *Sci. Rep.* **2012**, *2*, 755; b) N.-H. Cho, T.-C. Cheong, J. H. Min, J. H. Wu, S. J. Lee, D. Kim, J.-S. Yang, S. Kim, Y. K. Kim, S.-Y. Seong, *Nat. Nanotechnol.* **2011**, *6*, 675 – 682; c) Y. Deng, D. Qi, C. Deng, X. Zhang, D. Zhao, *J. Am. Chem. Soc.* **2007**, *129*, 28 – 29.
[13] a) A. Zylbersztejn, N. F. Mott, *Phys. Rev. B* **1975**, *11*, 4383 – 4395; b) S. S. N. Bharadwaja, C. Venkatasubramanian, N. Fieldhouse, S. Ashok, M. W. Horn, T. N. Jackson, *Appl. Phys. Lett.* **2009**, *94*, 222110.

Received: April 7, 2016
Published online: June 6, 2016

